Chinese Journal of Physiology 53(1): 52-61, 2010
DOI: 10.4077/CJP.2010.AMK015

Differences in the Pattern of Ventricular Activation in Small Rodents Determined by Morphological Organization of the Cardiac Ventricular Conduction System

Toon A.B. van Veen[1], Lisette E.G. Hubens[1], Jacques M.T. de Bakker[1, 2, 3], and Harold V.M. van Rijen[1]

[1]*Division of Heart and Lungs, Department of Medical Physiology, University Medical Center Utrecht, Utrecht*
[2]*Interuniversity Cardiology Institute of the Netherlands, Utrecht*
and
[3]*Heart Failure Research Center, Department of Experimental Cardiology, Academic Medical Center, Amsterdam, the Netherlands*

Abstract

Ventricular activation of the mouse heart differs significantly compared to activation in larger mammals. Knowledge of structural and functional characteristics of laboratory animals is essential for evaluation of results obtained from experiments. The present study was performed to evaluate whether the different pattern of activation is common to small rodents or unique for mice. Hearts of adult Wistar rats were isolated and Langendorff perfused. After removing the right and left ventricular free wall, extracellular activity of the septum and bundle branches (BB) was determined using a multi-terminal electrode harboring 247 terminals. Immunolabeling on cryosections was performed to assess expression and distribution of the gap junction proteins Connexin40 (Cx40), Cx43, Cx45, contractile (Desmin, α-actinin) and intercalated disk-related (N-cadherin, β-catenin) proteins. Collagen distribution was assessed by Sirius Red staining. Reconstruction of the left and right bundle branch (LBB and RBB) using immuno-labeling revealed that the LBB spreads all over the septal surface. The RBB too is broad, albeit to a lesser extend than LBB. A sheet of connective tissue electrically separates the common bundle and proximal BB from the septal working myocardium. Immunolabeling revealed clear differences between the conduction system and the working myocardium with respect to expression level and distribution of the different proteins analyzed. The morphological organization of the area resulted in an electrical activation pattern of the septum comparable to what is common in larger mammals: earliest activation at the midseptum *via* the bundle branches. From our data we conclude that the pattern of ventricular activation in the rat heart and the structure of the conduction system fit to data described for larger mammals and differ from the different pattern previously found in mouse heart.

Key Words: connexin, gap junction, conduction system, impulse propagation, mice, rats

Introduction

Impulse propagation throughout the heart depends on geometry of the tissue, electrical coupling between the cardiomyocytes and excitability of the cells. Geometry of the tissue includes cell-size and cell-shape, as well as non-excitable, insulating connective tissue. Propagation of the action potential to

Corresponding author: Toon A. B. van Veen, Ph.D., Division of Heart & Lungs, Department of Medical Physiology, University Medical Center Utrecht, Yalelaan 50, 3584 CM Utrecht, The Netherlands. Tel: 0031302538900, Fax: 0031302539036, E-mail: a.a.b.vanveen@umcutrecht.nl
Received: February 25, 2009; Revised: April 15, 2009; Accepted: June 18, 2009.
 ISSN : 0304-4920. http://www.cps.org.tw

neighboring myocytes depends on the functional expression of gap junction channels. Gap junction channels are intercellular channels that connect the cytoplasm of adjacent cells. Such channels are composed of hexagonally arranged connexin proteins which form a large family of highly related though functionally distinct isoforms (18). In between cardiomyocytes, including those that compose the conduction system, gap junctions can be composed of connexin40, (Cx40), Cx43 or Cx45 (reviewed in (20)). In the mammalian heart, Cx40 and Cx45 predominate in the conduction system, while Cx43 is the far most abundant isoform expressed in working myocardium. Recently, expression of a fourth isoform, Cx30.2, has been described in mouse heart where it is exclusively located in the AV-node (9), but this isoform could not be identified in the human heart (10).

In previous studies we have investigated how the various factors influence impulse propagation through the ventricular conduction system in mouse hearts under physiological conditions (23), and upon modulation of intercellular electrical coupling (1, 17), or action potential formation (22). Under physiological conditions, the sequence of ventricular activation in the mouse heart appeared to be significantly different from the pattern of activation as reported in larger mammals. Textbook physiology learns that in hearts of large mammals, impulse propagation through the common bundle (CB) proceeds into both bundle branches (BB), from which the impulse is conducted into apical direction. Connection of the specific conduction system to working myocardium only occurs at the Purkinje-muscle junction. First activation of the ventricular septal working myocardium (SWM) is commonly found halfway the septum. Following this sequence of activation, highly similar ventricular activation patterns derived from subsequential beats can be recorded (23).

In the mouse heart, impulse propagation through the CB preferentially activates the ventricular SWM already at the base rather than midseptally. This appears to be due to the absence of a continuous and isolating sheet of connective tissue at the interface between the CB and the interventricular septum. In larger hearts, this isolating sheet of connective tissue prevents activation of the septal myocardium and directs the electrical impulse into the BB. In the mouse heart, a peculiar connection between the CB and the septum gives rise to a different sequence of ventricular activation, resulting in irregular patterns of successive beats (23).

To unravel the molecular substrate underlying cardiac electrophysiology, multiple (mostly genetically modified) mouse models have been used to study pathophysiological alterations in relation to cardiac excitation, conduction and repolarization. To extrapolate the outcome of such studies to a higher level might be hampered by the observed aberrancies with respect to the electrical activation pattern in the mouse heart. To investigate whether the different pattern of activation is restricted to the mouse heart alone or more generalized to rodents, we performed a comparable study on rat hearts. Comparison of our previously published data on mouse heart with those obtained in this study implicates that, though evolutionary closely related, morphological organization and electrical activation of the rat heart is more comparable to that in larger mammals than to that in mouse hearts.

Materials and Methods

Animals

Commercially available adult Wistar rats (n = 8) between 4 and 6 months of age were used for the electrophysiological and immunohistochemical experiments. Experiments were performed according to the Dutch Experiments on Animals Act and the European Directive for the Protection of Vertebrate Animals Used for Experimental and Other Scientific Purposes (86/609/EU). The study complies with the *Guide for the Care and Use of Laboratory Animals* published by the US National Institutes of Health (No. 85-23, revised in 1996). The experiments were approved by the Animal Experiments Committee of Utrecht University.

Preparation of the Hearts

Rats were anaesthetized by an intraperitoneal injection of urethane (2.0 g/kg body weight). After opening of the chest, the heart was excised and submerged in ice-cold Tyrode's solution. Next, the heart was dissected from lungs and other tissue and the aorta was cannulated. Subsequently, the heart was connected to a custom built Langendorff perfusion setup and retrogradely perfused at 3°C with a perfusion pressure of 80 cm H_2O. Perfusion buffer composition was (in mM): NaCl 90, KCl 3.6, KH_2PO_4 0.92, $MgSO_4$ 0.92, $NaHCO_3$ 19.2, $CaCl_2$ 1.8, glucose 22, creatin 6, taurine 6, insulin 0.1 μM, gassed with 95% O_2 and 5% CO_2. In all experiments the heart started to beat immediately after initiating perfusion. Flow rate was approximately 10 ml/min. To prevent heat loss to the surroundings, the heart was placed against a heated (37°C) and continuously moisturized support.

Recording of Electrograms

Extracellular electrograms were recorded with a 247 points electrode (19 by 13 grid, inter-electrode distances of 0.3 mm), mounted in a micromanipulator.

Recordings were made in unipolar mode with regard to a reference electrode connected to the support of the heart. Electrograms were acquired using a custom built 256-channel data-acquisition system. Signals were bandpass filtered (low cut-off 0.16 Hz (12 dB), high cut-off 1 kHz (6 dB)), and digitized with 16 bits resolution at a bit step of 2 μV and a sampling frequency of 2 or 4 kHz. The input noise of the system was 4 μV (peak-peak). For septal measurements, the right and left ventricular free walls were removed and the electrode grid was positioned on the inter ventricular septum (IVS) just below the atrio-ventricular valves. Atrial pacing was performed at twice the stimulation threshold. Each stimulus train was composed of 16 basic stimuli (S1) of 150 ms, followed by one premature stimulus (S2) of 140 ms, which was decremented by 10 ms steps until the AV effective refractory period (AVERP) was reached.

Data Analysis

Activation maps were constructed from activation times, determined with custom written software based on Matlab (The Mathworks Inc., Natrick, MA, USA). The moment of maximal negative dV/dt in the unipolar electrograms was selected as the time of local activation. Activation times of at least 4 consecutive electrode terminals along lines perpendicular to intersecting isochronal lines were used to determine effective conduction velocity (CV). Statistical comparisons were performed using a paired Student's *t*-test, using SPSS 11 for Macintosh. Values are given as means ± standard error of mean. P values ≤ 0.05 were considered as statistically significant.

Immunohistochemistry and Histology

Following the electrophysiological recordings, hearts were rapidly frozen in liquid nitrogen and stored at –80°C. Frozen hearts were serially sectioned in a frontal plane ('four chamber view') or perpendicular to the long axis (transverse) to produce sections of 10 μm thickness. Multiple sections taken from different levels (frontal to dorsal) of the interventricular septum were incubated with primary antibodies directed against Cx40, Cx43, Cx45, α-actinin, β-catenin, desmin, N-cadherin and SCN5a as reported previously (21). Transversal sections taken from the midsection of the basis to apex axis were incubated with Cx40, Cx43 and SCN5a in order to delineate the bundle branches. After immunolabeling, sections were mounted in Vectashield (Vector Laboratories, Burlingame, CA, USA) and examined using a light microscope equipped for epifluorescence (Nikon Optiphot-2, Amstelveen, The Netherlands).

To evaluate the presence of connective tissue, sections serial to the ones used for antibody-labeling were stained with Picro Sirius red. Previously acquired 10 μm sections of wildtype mouse heart (C57B6, stored at –80°C) were processed in a similar fashion for a morphological comparison between mouse and rat, additional to data published before (23).

Antibodies

The following antibodies were used; rabbit polyclonal antibodies raised against Cx45 (kindly provided by Dr. T.H. Steinberg, Washington University, St. Louis, USA (12)), Cx40 (Chemicon, Temecula, CA, USA), N-cadherin (Sigma, St. Louis, MI, USA), SCN5a (Alomone labs, Jerusalem, Israel) and mouse monoclonal antibodies raised against Cx43 (Transduction Laboratories, Lexington, KY, USA), desmin (Sanbio, Uden, The Netherlands), α-actinin (Sigma, St. Louis, MI, USA) and β-catenin (Transduction Laboratories, Lexington, KY, USA). Secondary antibodies (Texas Red and FITC conjugated whole IgG) were purchased from Jackson Laboratories (West Grove, PA, USA).

Results

Delineation of the Ventricular Conduction System

In a similar fashion as described previously for mouse heart, we divided the interventricular septum of the rat heart in three regions; P1, P2 and P3 (23). P1 is located directly apical from the bifurcation of the CB (until 2.5 mm below the valves), P2 comprises the midsection (2.5-8.0 below the valves) and P3 the distal part of both BB and the Purkinje-fibers (from 8.0 mm below the valves into apical direction).

Expression profiles of several myocardial proteins proved to be useful tools to demarcate the ventricular conduction system apart from the SWM. Both in mice (Fig. 1A) and rats (Fig. 1G), desmin labeling of the ventricular conduction system appeared more intense compared to labeling of the SWM. Double labeling of the desmin stained section shown in Fig. 1A with Cx40 (Fig. 1B) shows that the highest intensity of desmin labeling correlates with Cx40 positive cells of the conduction system (LBB) in the mouse. On the other hand, double labeling of mouse heart sections with α-actinin (Fig. 1C) and Cx40 (Fig. 1D) revealed a lower intensity of α-actinin labeling in the ventricular conduction system (CB) compared to the SWM. A similar difference in intensity of α-actinin labeling was observed in rats (Fig. 1H). Control incubations using only the fluorescent secondary antibody excluded that the difference in intensity was caused by a-specific tissue-border labeling of the secondary antibody (data not shown).

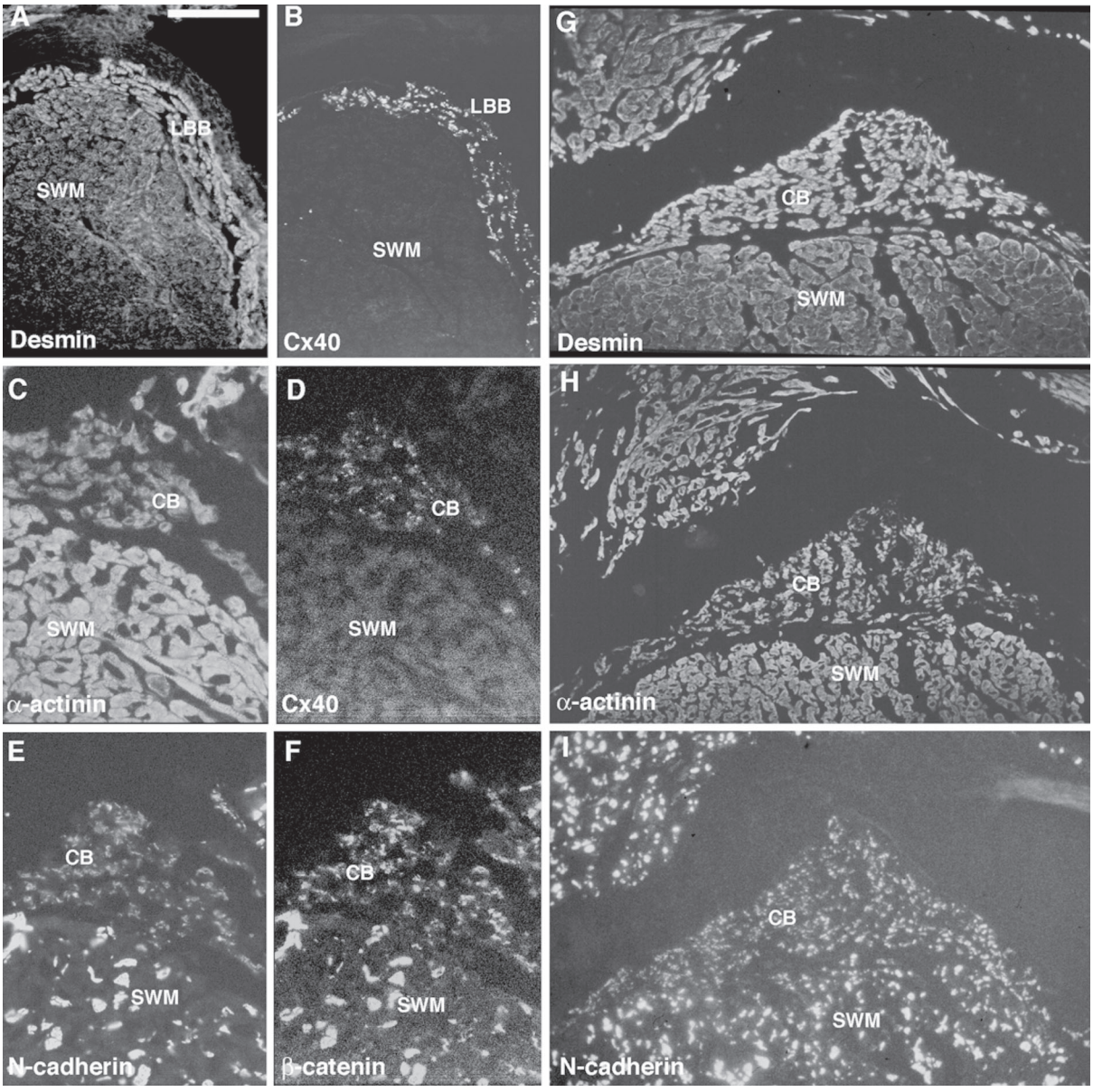

Fig. 1. Immuno-labeling of the interventricular septum focused on the common bundle (CB) and the proximal bundle branches (BB) in mouse (A-F) and rat (G-I). Double labeling of the indicated area with antibodies raised against desmin and Cx40 (separately depicted in A and B), of α-actinin and Cx40 (depicted in C and D), and of N-cadherin and β-catenin (depicted in E and F). G-I: labeling of the CB-SWM transition in rat heart using antibodies against desmin (G), α-actinin (H) and N-cadherin (I). Bar (indicated in A) = 100 μm in A, B, 150 μm in G, H, I and 50 μm in C, D, E, F. SWM = septal working myocardium, LBB = left bundle branch.

Labeling against N-cadherin, an intercalated disk (ID) associated component of the adherence junction, suggests that both in mice (Fig. 1E) and rats (Fig. 1I), IDs between myocytes of the ventricular conduction system are smaller compared to IDs between septal working myocardial cells. Double-labeling of the section shown in Fig. 1E with β-catenin, another ID related protein, further confirmed this observation in mouse heart (Fig. 1F).

In order to visualize the extensiveness of both BB in the rat heart, transversal sections taken from the midsection of P2 (about 5 mm below the bifurcation) were analyzed. Labeling with Cx40 antibodies allowed to compose the extension of both BB as shown in Fig. 2A (LBB) and 2C (RBB). In general, the LBB displayed a broad network of Cx40 positive fibers covering an average width of 2.5 mm. The typical example shown in Fig. 2A displays clear positive Cx40 labeling in the LBB while the SWM is negative. Fig. 2B highlights the area marked with an asterisk

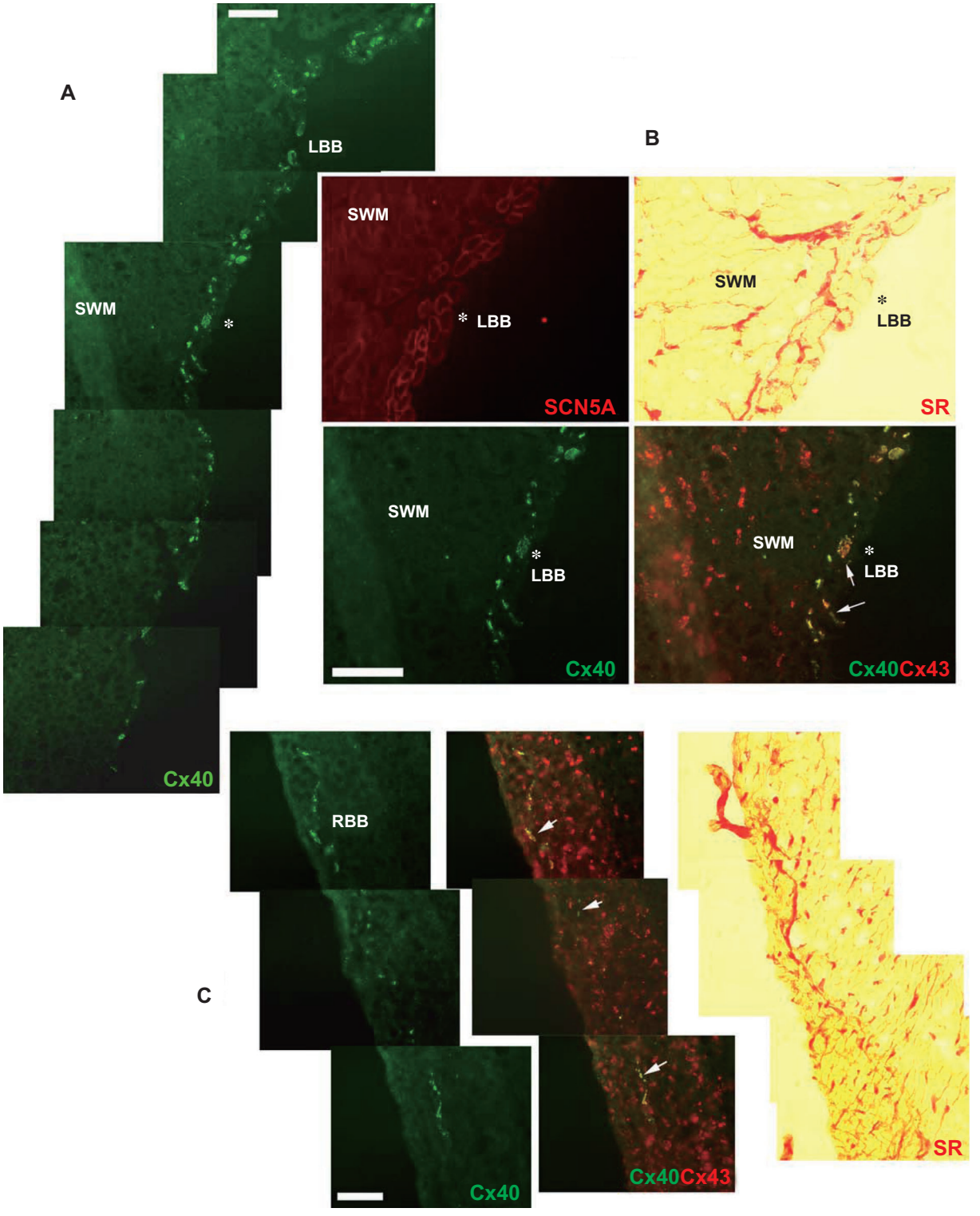

Fig. 2. Composition of the course of the left bundle branch (LBB, A and B) and right bundle branch (RBB) in rat heart. Sections used were sliced in a transversal direction and taken from a single plane section of the septum (middle of P2). A: Composition of the LBB on the left septal surface using immunolabeling against Cx40. Labeling indicates that the LBB covers the septum for about 2.5 mm in broadness. B: Immuno-labeling against SCN5a (left upper panel) revealed a higher intensity of SCN5a in the LBB when compared to the SWM. Labeling against Cx40 (left and right lower panel) and Cx43 (right lower panel). Arrows in the lower right panel indicate colocalization of Cx40 and Cx43 in the LBB. Picro-sirius red staining (SR) shows connective tissue within the LBB area (upper right panel). The asterisk in A and those in all panel of B indicate identical locations. C: Composition of the much smaller right bundle branch using antibodies against Cx40 (left and mid-panel) and Cx43 (mid-panel). SR staining of the area is shown in the most right panel. Bars represent 100 µm.

in Fig. 2A. Counterstaining of Cx40 with Cx43 antibodies revealed colocalization of Cx40 and Cx43 in the LBB (indicated with arrows). Sections serial to this one were labeled for SCN5a, (the alpha subunit of the cardiac sodium channel) or processed for Sirius Red (SR) staining of collagen. Besides the biomarkers discussed in Fig. 1, also SCN5a displayed a differential labeling intensity between the SWM and the LBB since cardiomyocytes of the LBB displayed a stronger intensity of labeling (left upper panel). SR staining revealed that although connective tissue (red color) was present between the myocytes of the BB and in between the BB and the SWM, the amount of connective tissue was not robust (right upper panel).

In contrast to the LBB, Cx40 labeling of the RBB (Fig. 2C) was detected in a much smaller area of the septal surface. In general, broadness of the RBB was restricted to approximately 1 mm while labeling intensity and the amount of positive spots were more restricted (left panel). Similar as described for the LBB, colocalization with Cx43 was found in the Cx40 positive cells (mid panel, arrows) while the degree of connective tissue was similar as in LBB (right panel).

Expression Pattern of Gap Junctions and Presence of Collagen

Cx43 is the exclusively observed connexin isoform in the SWM. In the CB, labeling of Cx40 (Fig. 3A) and Cx45 (Fig. 3B) could be detected while Cx43 appeared absent in this area. In contrast to the expression pattern previously described for mouse (23), Cx43 does not colocalize with Cx40 nor with Cx45 (Fig. 3A and 3B) at the transition of the CB and the septal working myocardium. Here, a narrow immunonegative space separates both regions. In the very proximal LBB (directly below the base in P1), colocalization of Cx43 with Cx40 is already detectable just apical from the bifurcation (Fig. 3D and 3E). Sirius Red staining of serial sections showed that the CB is isolated from the basal part of the SWM by a continuous sheet of connective tissue (arrows in Fig. 3C). Additionally, more connective tissue is found, surrounding the myocytes of the proximal BB (Fig. 3F). The area in between the two asterisks indicated in Fig. 3D and 3E, is similar to the area indicated in Fig. 3F.

Cellular Organization of Gap Junction Expression in the BB

Myocytes of the proximal BB differ in several aspects from SWM myocytes. As already displayed in Fig. 1I and 1D labeling profiles in myocytes of the BB are smaller than neighboring SWM cardiomyocytes while expression levels of several proteins differ between the two regions. Next to that, myocytes of the BB and those of the SWM express different connexins. Between ventricular and atrial cardiomyocytes, gap junctions are fairly exclusively located at the IDs forming the longitudinal cell borders (arrow in Fig. 4A). However, in rat BB, distribution of gap junctions differs from SWM cells. Although labeling in cells of the BB was also found at the longitudinal cell borders, profound diffuse labeling was detected over the entire cell length as displayed for Cx43/Cx40 in Fig. 4A and Cx43/Cx45 in Fig. 4B. Those double-labeling procedures also revealed that coexpression of the three connexin isoforms is present in the proximal BB. Identical observations were obtained from labeling on the RBB (data not shown). The aberrant labeling pattern (when compared to the SWM), appeared not to be restricted to the gap junction proteins as labeling against the adherence junction component N-cadherin (Fig. 4C), showed a comparable pattern as described for the Cxs. In contrast to the mouse BB, which also can be characterized by an aberrant distribution of gap junctions as compared to SWM, no small step-like ID structures as seen in mouse hearts (Fig. 4D and (23)), could be identified.

Conduction of the Electrical Impulse

For mapping of electrical activity of the rat septum, the electrode grid was positioned against the septal surface just below the atrio-ventricular valves (indicated in Fig. 5). Since the grid did not cover the septum completely, after the initial recordings, the grid was repositioned towards the apex in order to map electrical activity in this region too.

Representative electrograms are shown as recorded from each of the individual electrodes in the grid. BB activation maps were generated from the low amplitude electrical signal (red arrows) representing BB activation which preceded the large deflection (blue arrows) of SWM depolarization that was used to generate the septal activation maps.

Bundle branch recordings in rat revealed that there were no significant differences in conduction velocity ($n = 3$, $P = 0.82$) over the entire recorded distance (P1 and first half of P2). The amount of electrodes (interspaced by 300 μm) from which bundle branch signals could be recorded was compatible to broadness of both BB as deduced from immunohistochemical reconstructions (see Fig. 2). We were however unable to map electrical activity of the BB in the distal parts (apical part P2 and P3). Conduction velocity in the LBB was 52.5 ± 7.7 cm/s and in the RBB was 54.5 ± 3.9 cm/s. Rat septal activation maps made during sinus rhythm revealed that earliest activation (in red) was found in the midseptal region

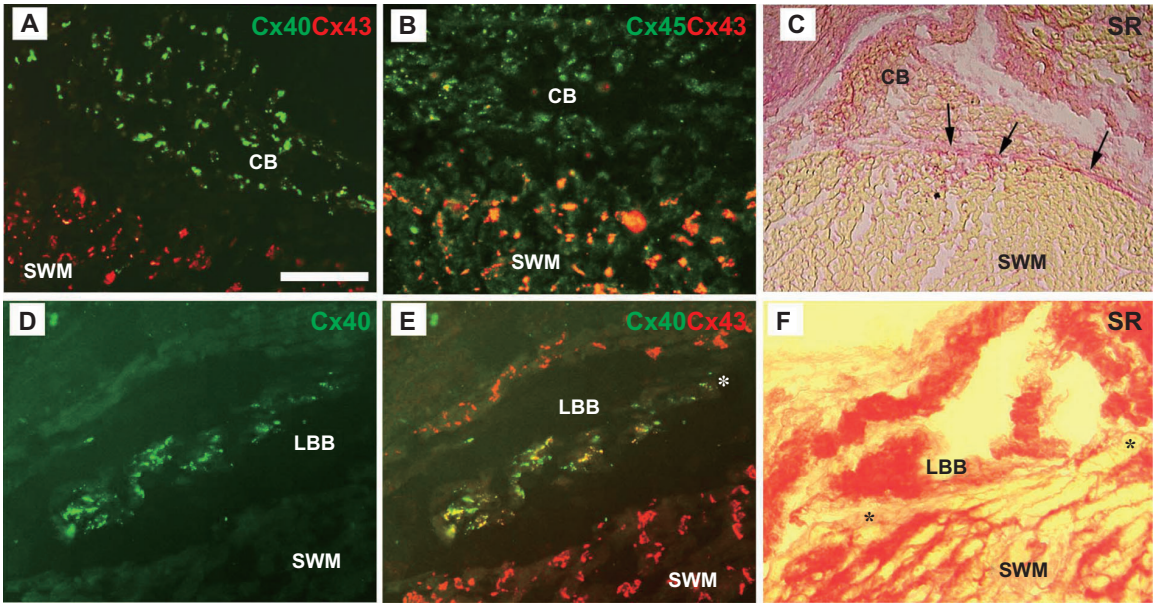

Fig. 3. Immuno-labeling (A, B, D, E) and Picro-sirius red staining (SR) of collagen (C, F) of the interventricular septum focused on the common bundle (CB) and the proximal left bundle branches (LBB) in rat. Cx40 (A) and Cx45 (B) are present in the CB where Cx43 is negative. In contrast Cx40, which is positive in the LBB but negative in the SWM (D), colocalizes with Cx43 within the LBB (E). SR staining revealed an insulating sheet of connective tissue in between the CB and the SWM (see arrows in C), while connective tissue was also profoundly present surrounding the LBB (F). Area in between the asterisks in D, E and F is similar. Bar (in A) = 100 µm in A, B, D, E, F and 150 µm in C. SWM = septal working myocardium.

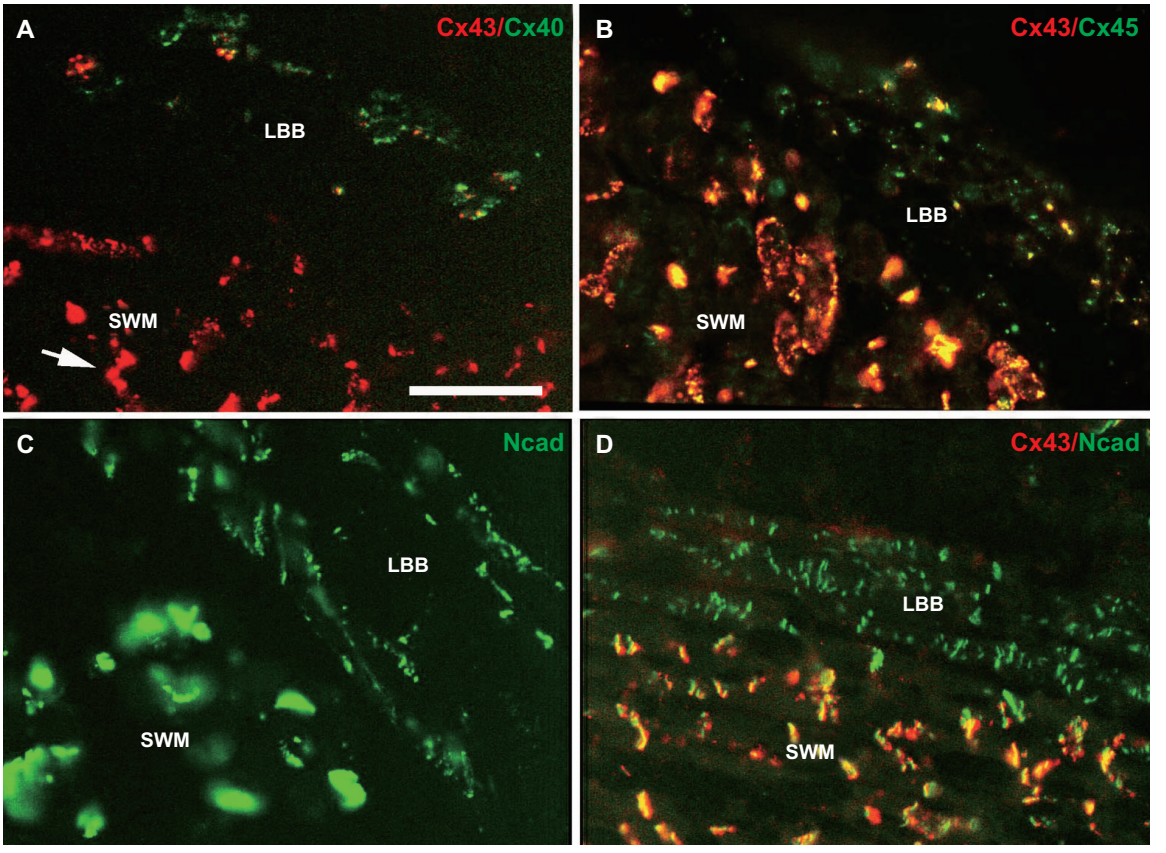

Fig. 4. Immuno-labeling of the interventricular septum focused on the very left proximal bundle branch (BB) in rat (A-C) and mouse (D). Double-labeling with antibodies against Cx40/Cx43 (A), Cx43/Cx45 (B), N-cadherin (C) and N-cadherin/Cx43 (D). Bar (indicated in A) = 50 µm in A, B, C, D. SWM = septal working myocardium, LBB = left bundle branch.

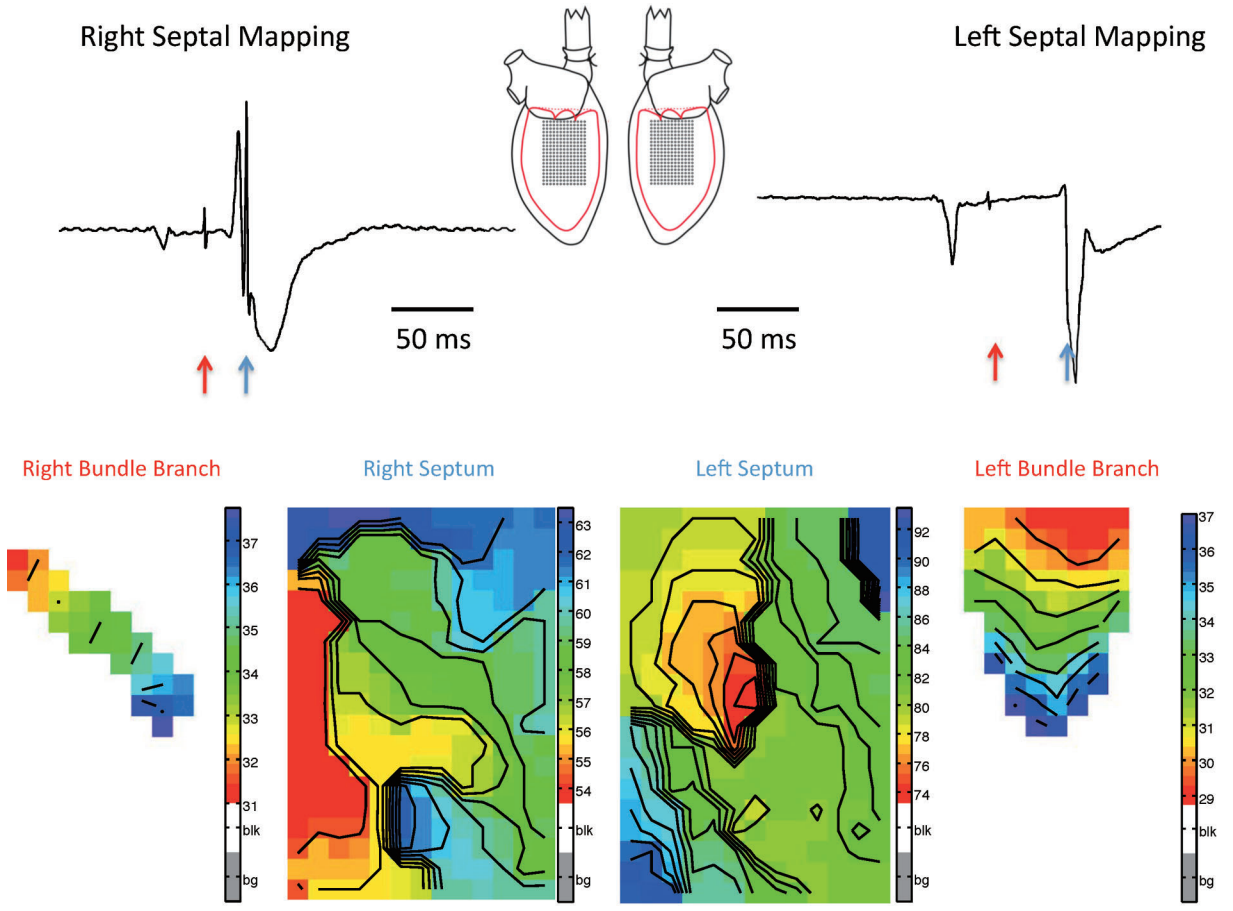

Fig. 5. Electrical activation mapping of the right and left rat septum. A schematic representation indicates the positioning of the electrode grid on the septum. Traces are representative recordings, which can be made with each of the 247 electrodes in the grid. From each signal the small bundle branch signal (red arrows) and the large septal deflection (blue arrows) were used to generate activation maps as shown in the lower panels. Red colors indicate earliest activation, blue colors latest activation. Black lines are isochrones at 1 ms intervals.

from which the activation spreads over the septum. This pattern of activation was found both at the left side and the right side. On both sides, activation maps generated from more than 10 subsequent beats displayed a high degree of similarity with identical spots of earliest activation.

Discussion

This study shows that: [1] the pattern of ventricular activation in rat heart aligns to that commonly found in larger mammals rather than to the pattern observed in mice. [2] The different patterns of ventricular activation in rats and mice can be explained by differences in the morphological organization of the conduction system. [3] Expression and distribution of various contractile and ID-associated proteins including the gap junction proteins Cx40, Cx43 and Cx45 differ between the bundle branches and working myocardium.

For every heartbeat, once generated in the sinus-node, a well controlled spatio-temporal propagation throughout the heart is facilitated by a highly orchestrated anatomical substrate. At the ventricular level, this anatomical organization can be separated in a conduction system (common bundle, bundle branches and Purkinje fibers) and the working myocardium. Important determinants within this substrate are the functional expression of gap junction channels (to electrically connect adjacent cardiomyocytes), ion channels (to regenerate the electrical signal once a myocyte is activated through its depolarized neighbor) and presence of electrically insulating connective tissue. Collagen forms the framework in which the myocardial cells are embedded to give the heart its rigid structure. In large mammals a sheet of connective tissue encloses the BBs, which electrically isolates the bundle from the SWM and as such prevents premature activation of the SWM. Consequently the action potential is propagated from the common bundle through the BBs in order to activate the ventricles and septum by the Purkinje system from left to right and

from apex to base (3, 5).

In a previous study, we investigated the morphological organization of the conduction system in mouse heart in relation to the pattern of electrical activation (23). The conclusion from this study was that the pattern of electrical activation in mouse heart is strikingly different from that in large mammals and that this was caused by delicate differences in morphological organization. To reveal whether these differences were common in small hearts of evolutionary related animals or restricted to mice only, the current study was performed.

The most important finding in this study relates to intrinsic differences in one of the determinants of the anatomical substrate for impulse propagation: the organization of connective tissue in the conduction system. In between the CB and the basis of the SWM a thin immuno-negative space could be detected where no gap junctions were present since it represented an insulating sheet of connective tissue. Also surrounding the proximal BB, significant amounts of connective tissue were detected that disabled a direct electrical connection to the SWM. This organization is comparable to that in larger mammals where a sheet of connective tissue electrically isolates the common bundle from the SWM in order to prevent premature activation of the SWM at the basis. In contrast, in mouse hearts Cx43 and Cx45 co-localize in the mentioned borderzone, which is facilitated by the fact that the thin sheet of connective tissue appeared discontinuous and penetrated by myocytes which physically connected to each other (23).

Besides a difference in organization of connective tissue, though maybe less important, also the expression of the gap junction protein Cx43 in the BBs is subject to small differences between rats and mice. While in both species Cx40 and Cx45 are expressed in the complete conduction system, expression of Cx43 in mouse BB does not colocalize with Cx40 and Cx45 until the level of P3, the very distal parts of the BB and the Purkinje fibers. In rats, Cx43 is already co-expressed at the very basal parts of the BB (just apical from the bifurcation). This expression of Cx43 in the proximal BB has previously been shown for larger mammals as human and cow. In these species, the proximal BB is separated from the septal working myocardium by an isolating sheet of connective tissue (14), comparable to what we show in this study on rats. Activation maps of the septum support the concept that the bundle is not connected to the myocardium at this level.

In general, Cx43 (atria and ventricles) and Cx40 (atria) in working myocardial myocytes are predominantly expressed in IDs at the longitudinal cell borders, where they colocalize with N-cadherin and desmoplakin (2, 15). This polarized distribution favors longitudinal over transverse conduction and thus gives rise to anisotropic conduction (19). In the BB however, expression of all three connexin isoforms but also of the adherence junction protein N-cadherin is different. Besides that labeling was identified at the longitudinal cell borders, profound diffuse labeling covered the complete sarcolemma. This labeling pattern, together with the already mentioned sheet of connective tissue surrounding the proximal conductive cells conforms to the distribution of Cx43 in the BB of human and cow (14). This implies also that the expression pattern in rat BB differs from the peculiar distribution of IDs in the BB of mouse heart (see Fig. 4 and (23)).

In addition to the aberrant organization of IDs in the BB, observations indicate that these myocytes are phenotypically different from working myocardial cells: [1] The diffuse labeling for Cx40, Cx43, Cx45 and N-cadherin in myocytes of the rat conduction system, has been described before in other cardiomyocyte phenotypes like neonatal and maturating myocytes (2, 11), dedifferentiating adult myocytes in culture (8), and in cardiomyopathic hearts (19). [2] Similar to embryonic stages of mouse heart (6), and adult bovine heart (14), also in adult rats and mice (see Fig. 1) differences exist between the expression levels of desmin and α-actinin in the conduction system and the SWM. [3] The increased expression level of the cardiac sodium channel (SCN5a) in the rat BB as compared to the SWM has also been observed in adult mouse heart (4, 16). Whether the phenotypical differences originate from differences in cellular differentiation during cardiac development (13), or from differences in the origin of the tissue (two different germ layers) (7), is still unresolved.

Similar as in mice, the LBB in rats is rather broad as it covers the majority of the left septal surface. On the right side however, the RBB covers a much larger area than found in mice where the RBB exists of only one or two tiny strands (Fig. 2 and (23)). In rat BB, conduction of the action potential is (equally) rapid over the entire length measured which fits with a homogeneous expression and distribution of gap junction proteins. In mice, despite slight intrinsic differences in expression/distribution of the gap junctions, propagation in the proximal BB is equally rapid as in rat, but reduced by half in the distal BB (23). A complete comparison between the velocities in rat and mouse BB is limited by the fact that in the current study we were unable to record BB signals in the very distal BB. We have to speculate to explain the underlying cause of this failure. It might be that in contrast to the mouse BB the distal BB in rat penetrates into deeper layers of the septum rather than run at the endocardial surface. It might well be that this aspect in combination with a high

degree of BB-sprouting results in too small electrical signals to be detected with our mapping electrode.

Electrical activation of the septal myocardium revealed that earliest activation occurred midseptal and latest activation at the basis (for both the left and right side). In mice, when measured at the right septal surface, earliest activation was predominantly observed at the basis and latest at the apex while at the left side both premature and bundle branch activation of the septum was detected (17, 23). In the current experiments, activation maps from more than ten subsequent beats were highly similar with identical sites (at the midseptum) of earliest activation. Thus, septal activation and morphology in rats conforms more to that of larger mammals than to a closely related family member as the mouse is.

Though the mouse is an indispensable model to study the invalidation of individual genes, knowledge that the conduction pathway in mouse heart is different when compared to that found in larger hearts (including rat heart) requires that extrapolation of studies on impulse propagation using knockout or transgenic mice should be made with caution. With upcoming new technologies that allow to equip complete hearts with exogenous genes (viral delivery) or to specifically silence genes (siRNA interference), the rat heart might become a strong extra tool to study aspects involved in patterns of electrical activation.

References

1. Alcolea, S., Jarry-Guichard, T., de Bakker, J., Gonzalez, D., Lamers, W., Coppen, S,. Barrio, L., Jongsma, H., Gros, D. and van Rijen, H. Replacement of connexin40 by connexin45 in the mouse: impact on cardiac electrical conduction. *Circ. Res.* 94: 100-109, 2004.
2. Angst, B.D., Khan, L.U.R., Severs, N.J., Whitely, K., Rothery, S., Thompson, R.P., Magee, A.I. and Gourdie, R.G. Dissociated spatial patterning of gap junctions and cell adhesion junctions during postnatal differentiation of ventricular myocardium. *Circ. Res*. 80: 88-94, 1997.
3. Burchell, H.B., Essex, H.E. and Pruitt, R.D. Studies on the spread of excitation through the ventricular myocardium. II. The ventricular septum. *Circulation* 6: 161-171, 1952.
4. Dominguez, J.N., de la Rosa, A., Navarro, F., Franco, D. and Aranega, A.E. Tissue distribution and subcellular localization of the cardiac sodium channel during mouse heart development. *Cardiovasc. Res.* 78: 45-52, 2008.
5. Durrer, D., van Dam, R.T., Freud, G.E., Janse, M.J., Meijler, F.L. and Arzbaecher, R.C. Total excitation of the isolated human heart. *Circulation* 41: 899-912, 1970.
6. Franco, D. and Icardo, J.M. Molecular characterization of the ventricular conduction system in the developing mouse heart: topographical correlation in normal and congenitally malformed hearts. *Cardiovasc. Res*. 49: 417-429, 2001.
7. Gorza, L. and Vitadello, M. Distribution of conduction system fibers in the developing and adult rabbit heart revealed by an antineurofilament antibody. *Circ. Res.* 65: 360-369, 1989.
8. Kostin, S., Hein, S., Bauer, E.P. and Schaper, J. Spatiotemporal development and distribution of intercellular junctions in adult rat cardiomyocytes in culture. *Circ. Res*. 85: 154-167, 1999.
9. Kreuzberg, M.M., Schrickel, J.W., Ghanem, A., Kim, J.S., Degen, J., Janssen-Bienhold, U., Lewalter, T., Tiemann, K. and Willecke, K. Connexin30.2 containing gap junction channels decelerate impulse propagation through the atrioventricular node. *Proc. Natl. Acad. Sci. U.S.A.* 103: 5959-5964, 2006.
10. Kreuzberg, M.M., Liebermann, M., Segschneider, S., Dobrowolski, R., Dobrzynski, H., Kaba, R., Rowlinson, G., Dupont, E., Severs, N.J. and Willecke, K. Human connexin31.9, unlike its orthologous protein connexin30.2 in the mouse, is not detectable in the human cardiac conduction system. *J. Mol. Cell. Cardiol*. 46: 553-559, 2009.
11. Kwak, B.R., van Kempen, M.J., Theveniau-Ruissy, M., Gros, D.B. and Jongsma, H.J. Connexin expression in cultured neonatal rat myocytes reflects the pattern of the intact ventricle. *Cardiovasc. Res.* 44: 370-380, 1999.
12. Lecanda, F., Towler, D.A., Ziambraras, K., Cheng, S.L., Koval, M., Steinberg, T.H. and Civitelli, R. Gap junctional communication modulates gene expression in osteoblastic cells. *Mol. Biol. Cell* 9: 2249-2258, 1998.
13. Moorman, A.F., de Jong, F., Denyn, M.M. and Lamers, W.H. Development of the cardiac conduction system. *Circ. Res*. 82: 629-644, 1998.
14. Oosthoek, P.W., Viragh, S., Lamers, W.H. and Moorman, A.F. Immunohistochemical delineation of the conduction system. II: The atrioventricular node and Purkinje fibers. *Circ. Res*. 73: 482-491, 1993.
15. Peters, N.S., Severs, N.J., Rothery, S.M., Lincoln, C., Yacoub, M.H. and Green CR. Spatiotemporal relation between gap junctions and fascia adherens junctions during postnatal development of human ventricular myocardium. *Circulation* 90: 713-725, 1994.
16. Remme, C.A., Verkerk, A.O., Aanhanen, W., Hoogaards, W.M.H., Scicluna, B.P., van den Hoff, M.J.B., Wilde, A.A.M., van Veen, T.A.B., Veldkamp, M.W. and de Bakker, J.M.T. The cardiac sodium channel displays differential distribution in the conduction system and transmural heterogeneity in the murine ventricular myocardium. *Basic Res. Cardiol*. 2009, in press.
17. van Rijen, H.V., van Veen, T.A., van Kempen, M.J., Wilms-Schopman, F.J., Potse, M., Krueger, O., Willecke, K., Opthof, T., Jongsma, H.J. and de Bakker, J.M. Impaired conduction in the bundle branches of mouse hearts lacking the gap junction protein connexin40. *Circulation* 103: 1591-1598, 2001.
18. Sohl, G. and Willecke, K. Gap junctions and the connexin protein family. *Cardiovasc. Res.* 62: 228-232, 2004.
19. Uzzaman, M., Honjo, H., Takagishi, Y., Emdad, L., Magee, A.I., Severs, N.J. and Kodama, I. Remodeling of gap junctional coupling in hypertrophied right ventricles of rats with monocrotaline-induced pulmonary hypertension. *Circ. Res*. 86: 871-878, 2000.
20. van Veen, T.A., van Rijen, H.V. and Opthof, T. Cardiac gap junction channels: modulation of expression and channel properties. *Cardiovasc. Res.* 51: 217-229, 2001.
21. van Veen, T.A., van Rijen, H.V., Wiegerinck, R.F., Opthof, T., Colbert, M.C., Clement, S., de Bakker, J.M. and Jongsma, H.J. Remodeling of gap junctions in mouse hearts hypertrophied by forced retinoic acid signaling. *J. Mol. Cell. Cardiol*. 34: 1411-1423, 2002.
22. van Veen, T.A., Stein, M,. Royer, A., Le Quang, K., Charpentier, F., Colledge, W.H., Huang, C.L., Wilders, R., Grace, A.A. and Escande, D. Impaired impulse propagation in *Scn5a*-knockout mice: combined contribution of excitability, connexin expression, and tissue architecture in relation to aging. *Circulation* 112: 1927-1935, 2005.
23. van Veen, T.A., van Rijen, H.V., van Kempen, M.J., Miquerol, L., Opthof, T., Gros, D., Vos, M.A., Jongsma, H.J. and de Bakker, J.M. Discontinuous conduction in mouse bundle branches is caused by bundle-branch architecture. *Circulation* 112: 2235-2244, 2005.